CRYSTAL STRUCTURES OF $Ti_{50}Ni_{50-x}Cu_X$ SHAPE MEMORY ALLOYS INVESTIGATED BY DFT CALCULATIONS

Liangliang Gou[*], Yong Liu [†], Teng Yong Ng [†]

[*] School of Mechanical and Aerospace Engineering, Nanyang Technological University
50 Nanyang Avenue, Singapore 639798
LGOU1@e.ntu.edu.sg

[†] School of Mechanical and Aerospace Engineering, Nanyang Technological University
50 Nanyang Avenue, Singapore 639798
MLiuY@ntu.edu.sg MTYNg@ntu.edu.sg

Key words: Shape-Memory Alloys, Density Functional Theory, Phase Transformation, Electronic Structure, Phase Stability.

Summary: *The martensite crystal structures and electronic structures of $Ti_{50}Ni_{50-x}Cu_x$ (x = 0, 5, 12.5, 15, 18.75, 20, 25) shape memory alloys are investigated using density functional theory (DFT). It is found that, by introduction of Cu atoms into TiNi martensite crystal, the lattice parameters (a and c) and the monoclinic angle decrease, while the lattice parameter b increases. When Cu content is increased to around 20 at%, an orthorhombic crystal structure is formed which agrees well with reported experimental observations. In particular, by introduction of Cu atoms into TiNi martensite crystal, Ti and Ni/Cu atoms move significantly along x-axis but insignificantly along y-axis and z-axis for all alloys examined. As a result, the distance between two Ni/Cu atoms increases while the Ti atoms get closer along x-axis, which is responsible for the decrease in the monoclinic angle. With increasing Cu content, fewer electrons were transferred from Ti to Ni in comparison with that in binary TiNi alloys, leading to a weaker interaction between them, which results in an increase of bond length. As the movements of both Ti and Ni/Cu atoms along x-axis are continuous, the monoclinic angle decreases gradually without dramatic change.*

1 INTRODUCTION

TiNi-based shape memory alloys (SMAs) have been widely used in the aerospace and biomedical fields because of their superior shape memory effect (SME), high superelasticity as well as favorable biocompatibility [1-5]. In order to fulfill the requirement of high response frequency in automotive and aerospace industries, TiNiCu SMAs in which Cu substitutes for Ni, have been widely studied owing to their narrow martensitic transformation (MT) temperature hysteresis in comparison with TiNi binary alloys [6-9]. In order to design new SMAs possessing very small transformation temperature hysteresis, understanding the effect of alloying on martensite structures is of vital importance. Previously reported works have studied the effects of Cu content on transformation temperature [10], microstructure [7, 8, 11-13], stress-strain characteristic and fatigue life [14-16], as well as applications as actuators [5, 17]. Earlier study has found that the Cu content in TiNiCu alloys has little

influence on the MT temperature but obvious effect on the MT pathway [11, 12, 18]. TiNiCu alloys with Cu content of less than 7.5 at% are known to show the B2→B19′ transformation. For the alloys with Cu content between 7.5 at% and 15 at%, there is a B2→B19→B19′ transformation, and for Cu ≥ 15 at%, a direct B2→B19 transformation takes place. Meanwhile, the transformation temperature hysteresis becomes smaller with increasing Cu content in TiNiCu alloy [7, 8, 10].

With the quick progress in high performance computing, the first principle density functional theory (DFT) has become one of the most broadly used approaches to investigate the crystal structures of SMAs at the quantum level [19-21]. Using the DFT method, a base-centred orthorhombic (BCO) structure with 107 ° monoclinic angle was reported by Huang et al. [22] in TiNi martensite, which is significantly different from the experimental reported value of 96.8 °. A new martensite structure in TiNi indicated as B19″ phase was predicted by Vishnu et al. [23] using a SeqQuest code based on the DFT.

In order to effectively design SMAs with required transformation hysteresis, understanding the atomic displacement and subsequent crystal structure transition as a result of alloying is of primary importance. However, the mechanism of Cu addition in modifying the martensite crystal structure is not clearly understood. In the present study, in order to determine how Cu content affects the martensite crystal structures of TiNiCu alloys, a first principle investigation on the atomic displacement of martensitic $Ti_{50}Ni_{50-x}Cu_x$ (x = 0, 5, 12.5, 15, 18.75, 20, 25) alloys has been performed. The results presented in this research may provide an insight for a better understanding of the transformation hysteresis in TiNiCu SMAs.

2 COMPUTATION METHODOLOGY

In this research, all calculations are carried out with generalized gradient approximation (GGA) of Perdew, Burke and Ernzerhof (PBE) [24] based on the DFT method as implemented in the CASTEP code [25, 26]. The cutoff energy of the plane wave was set to 1000 eV to ensure the accuracy. The integrations in the Brillouin zone were performed on a grid of 9×6×6 Monkhorst-Pack set. The convergence tolerance of energy, maximum force, maximum stress and maximum displacement were set to be $5.0×10^{-6}$ eV/atom, 0.01 eV/Å, 0.02 GPa and $5.0×10^{-4}$ Å, respectively. The ultrasoft pseudo-potentials were used to represent all ions. Pseudo atomic calculations performed for Ti, Ni and Cu are $3s^2 3p^6 3d^2 4s^2$, $3d^8 4s^2$ and $3d^{10} 4s^1$, respectively.

The martensite crystal structures of TiNiCu alloys with different Cu contents have been reported [22, 27-31] and are listed in Table 1. The B19 and B19′ phases were observed in experiments, while the BCO structure was obtained from computational calculations. In the present calculations, all initial crystal structures were set to monoclinic structures, i.e. B19′ phase. The original atomic positions of Ni and Ti were taken as x = 0.0525, y = 0.25, z = 0.693 and x = 0.4726, y = 0.25, z = 0.221, respectively [32].

Alloy	Phase	a (Å)	b (Å)	c (Å)	β (°)	Ref.
$Ti_{50}Ni_{50}$	BCO (Comp.)	2.94	3.997	4.936	107.0	[22]
$Ti_{50}Ni_{50}$	B19′-Monoclinic (Exp.)	2.89	4.12	4.62	96.5	[27, 28]
$Ti_{50}Ni_{30}Cu_{20}$	B19-Orthorhombic (Exp.)	2.88	4.28	4.52	--	[27, 28]

Table 1. Lattice parameters of, B19, B19′ and BCO from previous experimental and theoretical work.

In this research, all TiNiCu structures were optimized in two different methods, which are Supercell Method (SM) and Virtual Crystal Method (VCM), to ensure the accuracy of the results for crystal structures, and the calculation results were cross-checked. In order to obtain and visualize the atomic displacements in TiNiCu alloys with different Cu contents, the same unit cell has been used and all TiNiCu initial structures were optimized by the Virtual Crystal Method (VCM) [33].

3 RESULTS AND DISCUSSIONS

The calculated lattice parameters, through both SM and VCM, as a function of Cu content in TiNiCu alloys are shown in Figure 1. It can be observed that with increasing Cu content, the lattice parameters a and c decrease while the lattice parameter b increases. The results from these two methods are quite similar and the trends are identical. As the present calculation results agree well with the reported experimental observations [8, 10-12], it can be stated that the calculation results are accurate and trustworthy. It also shows that the lattice parameters of TiNiCu alloys are affected significantly by Cu content.
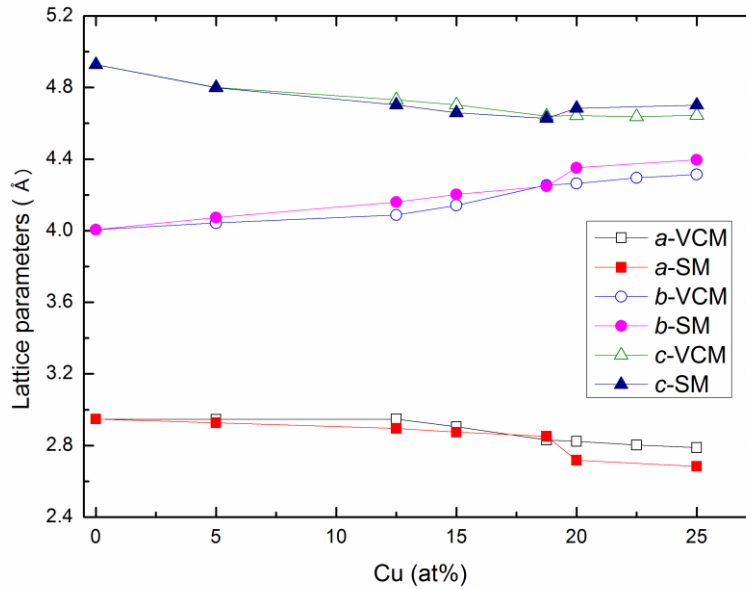

Figure 1. Variation of lattice parameters with different Cu content.

The monoclinic angle (β) and unit cell volume, as a function of Cu content in TiNiCu alloys, obtained through both SM and VCM are presented in Figure 2. From this figure, it can be seen that by increasing Cu content, the monoclinic angle (β) decreases gradually. When Cu content is between 0 at% and 18.75 at%, the stable martensite structure is monoclinic as B19′ phase. However, the B19 phase with orthorhombic structure is presented when the Cu content is increased to 20 at%, which are consistent with experimental observations. From Figure 2, it also can be observed that the unit cell volumes of the TiNiCu alloys remain stable with different Cu content.
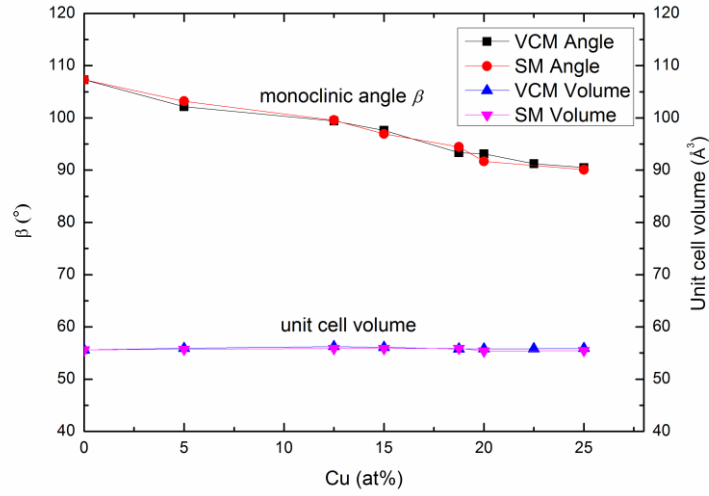
3

Figure 2. Variation of unit cell volume and monoclinic angle with different Cu content.

The calculated Mulliken charge transfer with different Cu content, are shown in Table 2. For binary NiTi alloy, it can be considered as a TiNiCu alloy containing 0 at% Cu. As shown in Table 2, with increasing Cu content, more electrons escape from the Ti atoms when compared with equiatomic TiNi binary alloy. As the ability of Cu atom to attract electrons is stronger than Ni, more charge transfer to Cu atoms than to Ni atoms was observed.

Alloys	Charges (e)		
	Ti	Ni	Cu
$Ti_{50}Ni_{50}$	0.365	-0.365	---
$Ti_{50}Ni_{45}Cu_5$	0.399	-0.348	-0.85
$Ti_{50}Ni_{37.5}Cu_{12.5}$	0.445	-0.323	-0.82
$Ti_{50}Ni_{35}Cu_{15}$	0.464	-0.3157	-0.81
$Ti_{50}Ni_{31.25}Cu_{18.75}$	0.495	-0.294	-0.83
$Ti_{50}Ni_{30}Cu_{20}$	0.496	-0.273	-0.83
$Ti_{50}Ni_{25}Cu_{25}$	0.54	-0.23	-0.85

Table 2. Calculated charge transfer per atom in TiNiCu alloys.

The calculated atomic positions of Ti and Ni/Cu as a result of Cu addition are listed in Table 3, in which reported experimental data are also included. From Table 3, it can be clearly observed that in the *x*-direction, the displacements of Ni/Cu and Ti atoms are clearly evident. Increasing Cu content leads to a displacement of Ni/Cu atom along the [$\bar{1}$00] direction and Ti atom in the [100] direction. Both Ni/Cu and Ti atoms remain unshifted in the [010] direction with increasing Cu content. The displacements of Ni/Cu and Ti atoms along the [001] direction are relatively small in all the alloys considered here. Since the Ni/Cu and Ti atoms remain unchanged along the [010] direction, it can be stated that all the atomic

displacements have occurred within the (010) plane. The schematic projections of the crystal structures along the *y*-axis for TiNiCu alloys containing different Cu contents are illustrated in Figure 3. The positions of Ni/Cu site (blue) and Ti site (grey) along '*a*' and '*c*' lattice parameters with respect to the binary alloy have been indicated. The dashed circles represent the original positions of Ni and Ti atoms in the computational $Ti_{50}Ni_{50}$ B19′ structure.

Alloys	Atomic parameter (Ni/Cu)			Atomic parameter (Ti)		
	x	*y*	*z*	*x*	*y*	*z*
$Ti_{50}Ni_{50}$ (Exp.)	0.0525	0.25	0.693	0.4726	0.25	0.221
$Ti_{50}Ni_{50}$ (Comp.)	0.08978	0.25	0.670962	0.351818	0.25	0.215147
$Ti_{50}Ni_{45}Cu_5$	0.0639	0.25	0.67	0.38695	0.25	0.215
$Ti_{50}Ni_{37.5}Cu_{12.5}$	0.0471	0.25	0.6687	0.402645	0.25	0.21339
$Ti_{50}Ni_{35}Cu_{15}$	0.0349	0.25	0.670517	0.416639	0.25	0.212366
$Ti_{50}Ni_{31.25}Cu_{18.75}$	0.0126242	0.25	0.677317	0.460799	0.25	0.213376
$Ti_{50}Ni_{30}Cu_{20}$	0.0116357	0.25	0.677294	0.462048	0.25	0.212587
$Ti_{50}Ni_{25}Cu_{25}$	-0.0019362	0.25	0.67934	0.506478	0.25	0.211795

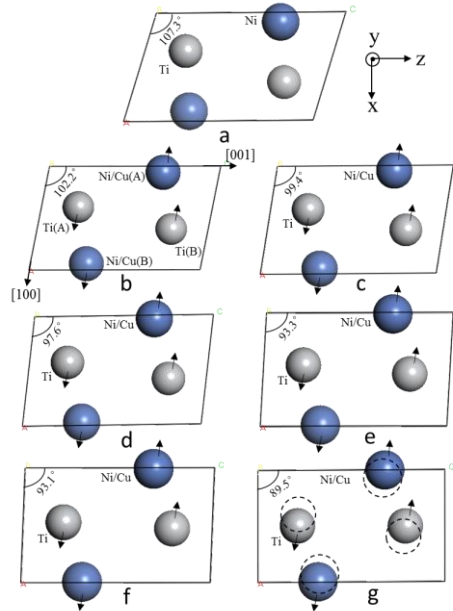Table 3. Atomic parameters (*x*, *y*, *z*) of Ti and Ni in TiNiCu alloys.

Figure 3. Projections of the martensite crystal structures along <010> direction of (a) binary $Ti_{50}Ni_{50}$; (b) $Ti_{50}Ni_{45}Cu_5$; (c) $Ti_{50}Ni_{37.5}Cu_{12.5}$; (d) $Ti_{50}Ni_{35}Cu_{15}$; (e) $Ti_{50}Ni_{31.25}Cu_{18.75}$; (f) $Ti_{50}Ni_{30}Cu_{20}$ and (g) $Ti_{50}Ni_{25}Cu_{25}$, comparing the typical relative average positions of Ni site (blue) and Ti site (grey) along '*a*' and '*c*' lattice parameters with respect to the binary alloy.

The crystal structure is determined by the atomic arrangements in crystalline solids. With increasing Cu content, the distance between the two Ni/Cu atoms increases along the *x*-axis,

while that between the Ti atoms decreases. Specifically for the Ni/Cu atom, when Cu content reaches 25 at%, the x-parameter is near zero. This form of atomic displacements within the (010) plane leads to a rotation of the (100) plane. As a result, the crystal structure changes from monoclinic (B19′) to orthorhombic (B19).

Moreover, this change is gradual. From Table 3, it can be clearly observed that the displacements of both Ti and Ni/Cu atoms in the x-direction are continuous, which results in a continuous change of the monoclinic angle and lattice parameters, leading to successive changes in the crystal structure. Thus, it can be surmised that, with increasing Cu content in TiNiCu alloys, the change in the martensite crystal structure from monoclinic B19′ to orthorhombic B19 is not dramatic but gradual.

Accommodation of Cu in the monoclinic martensitic TiNi takes place by substitution of Ni atom, and it is assumed that replacements are controlled primarily by the size mismatch of Cu [34]. The atomic radii of Ti, Ni and Cu are 1.45 Å, 1.29 Å and 1.28 Å, respectively. As the atomic radii of Cu is slightly smaller than that of Ni, the size mismatch is not significant, which is consistent with previous observation that there is no dramatic change of crystal structure when substituting Cu in TiNiCu martensitic alloys.

4 CONCLUSIONS

The present research has investigated the stable martensite crystal structure, electronic structure and atomic positions of $Ti_{50}Ni_{50-x}Cu_x$ (x = 0, 5, 12.5, 15, 18.75, 20, 25) alloys using DFT. The following conclusions can be drawn:

1. With increasing Cu content in TiNiCu alloys, the martensite lattice parameters a and c and the monoclinic angle decrease, while the lattice parameter b increases. When Cu content reaches to 20 at%, an orthorhombic crystal structure is presented. The computational results are in good agreement with experimental observations.

2. As a result of Cu addition to TiNi, the shifting of Ti and Ni/Cu atoms along the x-axis is clearly evident, but minimal along the y and z axes. With increasing Cu content, the distance between two Ni/Cu atoms increases along the x-axis while the Ti atoms become closer, which is responsible for the rotation of the (100) plane, leading to a decrease in the monoclinic angle.

3. With increasing Cu content, more electrons escaped from the Ti atoms and fewer charge transfer from Ti to Ni was observed as compared to that in binary NiTi alloys.

4. Since the atomic radius of Cu are very similar to those of Ni, the displacements of both Ti and Ni/Cu atoms along the x-axis are progressive, indicating no dramatic change in TiNiCu martensite crystal structures. Thus, the unit cell volumes of TiNiCu martensite structures remain stable with different Cu contents.

5. Since the present computational results agree well with previous experimental observation, this numerical approach provides a new avenue for investigating the effect of alloying on the crystal structure change in SMAs, and offers reasonable predictions.

REFERENCES

[1] K. Otsuka, X. Ren, Physical metallurgy of Ti–Ni-based shape memory alloys. *Progress in Materials Science*, **50**, 511-678, 2005.

[2] C.P. Frick, A.M. Ortega, J. Tyber, K. Gall, H.J. Maier, Multiscale structure and properties of cast and deformation processed polycrystalline NiTi shape-memory alloys. *Metallurgical and Materials Transactions A,* **35**, 2013-2025, 2004.

[3] S.H. Chang, W.C. Chiu, Selective leaching and surface properties of Ti50Ni50-xCux (x= 0-20 at.%) shape memory alloys for biomedical applications. *Applied Surface Science,* **324**, 106-113, 2015.

[4] M. Es-Souni, H. Fischer-Brandies, Assessing the biocompatibility of NiTi shape memory alloys used for medical applications. *Analytical and Bioanalytical Chemistry*, **381**, 557-567, 2005.

[5] C. Grossmann, J. Frenzel, V. Sampath, T. Depka, G. Eggeler, Elementary transformation and deformation processes and the cyclic stability of NiTi and NiTiCu shape memory spring actuators. *Metallurgical and Materials Transactions A,* **40**, 2530-2544, 2009.

[6] T.B. Massalski, J.L. Murray, L.H. Bennet, H. Baker, Binary alloy phase diagrams. *ASM International,* **550**, 173, 1986.

[7] T. Saburi, Y. Watanabe, S. Nenno, Morphological characteristics of the orthorhombic martensite in a shape memory Ti-Ni-Cu alloy. *ISIJ International*, **29**, 405-411, 1989.

[8] T.H. Nam, T. Saburi, K. Shimizu, Cu-content dependence of shape memory characteristics in Ti-Ni-Cu alloys. *Materials Transactions, JIM,* **31**, 959-967, 1990.

[9] K.N. Lin, S.K. Wu, Multi-stage transformation in annealed Ni-rich Ti49Ni41Cu10 shape memory alloy. *Intermetallics*, **18**, 87-91, 2010.

[10] K. Otsuka, X. Ren, Recent developments in the research of shape memory alloys. *Intermetallics*, **7**, 511-528, 1999.

[11] W. Tang, R. Sandström, Z. Wei, S. Miyazaki, Experimental investigation and thermodynamic calculation of the Ti-Ni-Cu shape memory alloys. *Metallurgical and Materials Transactions A,* **31**, 2423-2430, 2000.

[12] T. Tadaki, C. Wayman, Electron microscopy studies of martensitic transformations in Ti50Ni50−xCux alloys. Part I. Compositional dependence of one-third reflections from the matrix phase. *Metallography*, **15**, 233-245, 1982.

[13] Z. L. Xie, J. Van Humbeeck, Y. Liu, L. Delaey, TEM study of Ti50Ni25Cu25 melt spun ribbons. *Scripta Materialia*, **37**, 363-371, 1997.

[14] B. Strnadel, S. Ohashi, H. Ohtsuka, T. Ishihara, S. Miyazaki, Cyclic stress-strain characteristics of TiNi and TiNiCu shape memory alloys. *Materials Science and Engineering A*, **202**, 148-156, 1995.

[15] B. Strnadel, S. Ohashi, H. Ohtsuka, S. Miyazaki, T. Ishihara, Effect of mechanical cycling on the pseudoelasticity characteristics of TiNi and TiNiCu alloys. *Materials Science and Engineering A,* **203**, 187-196, 1995.

[16] S. Miyazaki, K. Mizukoshi, T. Ueki, T. Sakuma, Y. Liu, Fatigue life of Ti–50 at.% Ni and Ti–40Ni–10Cu (at.%) shape memory alloy wires. *Materials Science and Engineering A,* **273**, 658-663, 1999.

[17] C. Grossmann, J. Frenzel, V. Sampath, T. Depka, A. Oppenkowski, C. Somsen, Processing and property assessment of NiTi and NiTiCu shape memory actuator springs. *Materialwissenschaft und Werkstofftechnik,* **39**, 499-510, 2008.

[18] T.H. Nam, T. Saburi, Y. Kawamura, K.i. Shimizu, Shape Memory Characteristics Associated With the B2<-> B19 and B19<-> B19' Transformations in a Ti--40 Ni--10 Cu(at.%) Alloy. *Materials Transactions, JIM,* **31** 262-269, 1990.

[19] W. Koch, M.C. Holthausen, *A chemist's guide to density functional theory.* Wiley-VCH, New York, 2001.

[20] P. Hohenberg, W. Kohn, Inhomogeneous electron gas. *Physical Review*, **136**, B864, 1964.

[21] W. Kohn, L.J. Sham, Self-consistent equations including exchange and correlation effects. *Physical Review A*, **140**, A1133, 1965.

[22] X. Huang, G.J. Ackland, K.M. Rabe, Crystal structures and shape-memory behaviour of NiTi. *Nature Materials,* **2**, 307-311, 2003.

[23] K. Guda Vishnu, A. Strachan, Phase stability and transformations in NiTi from density functional theory calculations. *Acta Materialia,* **58**, 745-752, 2010.

[24] J.P. Perdew, K. Burke, M. Ernzerhof, Generalized gradient approximation made simple. *Physical Review Letters*, **77**, 3865-3868, 1996.

[25] M.C. Payne, M.P. Teter, D.C. Allan, T. Arias, J. Joannopoulos, Iterative minimization techniques for ab initio total-energy calculations: molecular dynamics and conjugate gradients. *Reviews of Modern Physics,* **64**, 1045-1097, 1992.

[26] S.J. Clark, M.D. Segall, C.J. Pickard, P.J. Hasnip, M.I.J. Probert, K. Refson, First principles methods using CASTEP. *Zeitschrift fur Kristallograhie,* **220**, 567-570, 2005.

[27] T.H. Nam, T. Saburi, Y. Nakata, K. Shimizu, Shape memory characteristics and lattice deformation in Ti-Ni-Cu alloys. *Materials Transactions, JIM,* **31**, 1050-1056, 1990.

[28] R. Bricknell, K. Melton, O. Mercier, The structure of NiTiCu shape memory alloys. *Metallurgical and Materials Transactions A,* **10**, 693-697, 1979.

[29] H. Rösner, P. Schloßmacher, A. Shelyakov, A. Glezer, The influence of coherent ticu plate-like precipitates on the thermoelastic martensitic transformation in melt-spun Ti50Ni25Cu25 shape memory alloys. *Acta Materialia,* **49**, 1541-1548, 2001.

[30] Z. Xie, G. Cheng, Y. Liu, Microstructure and texture development in Ti50Ni25Cu25 melt-spun ribbon. *Acta Materialia,* **55**, 361-369, 2007.

[31] Y. Tong, Y. Liu, Z. Xie, M. Zarinejad, Effect of precipitation on the shape memory effect of Ti50Ni25Cu25 melt-spun ribbon. *Acta Materialia,* **56**, 1721-1732, 2008.

[32] Y. Liu, Z. Xie, Twinning and detwinning of< 0 1 1> type II twin in shape memory alloy. *Acta Materialia,* **51**, 5529-5543, 2003.

[33] S.H. Jhi, J. Ihm, S.G. Louie, M.L. Cohen, Electronic mechanism of hardness enhancement in transition-metal carbonitrides. *Nature,* **399**, 132-134, 1999.

[34] M. Zarinejad, Y. Liu, T.J. White, The crystal chemistry of martensite in NiTiHf shape memory alloys. *Intermetallics*, **16**, 876-883, 2008.